Published OnlineFirst January 2, 2014; DOI: 10.1158/0008-5472.CAN-13-1955

Cancer Research

Unbiased Compound Screening Identifies Unexpected Drug Sensitivities and Novel Treatment Options for Gastrointestinal Stromal Tumors

Sergei Boichuk, Derek J. Lee, Keith R. Mehalek, et al.

Cancer Res 2014;74:1200-1213. Published OnlineFirst January 2, 2014.

Published OnlineFirst January 2, 2014; DOI: 10.1158/0008-5472.CAN-13-1955

Therapeutics, Targets, and Chemical Biology

Cancer Research

Unbiased Compound Screening Identifies Unexpected Drug Sensitivities and Novel Treatment Options for Gastrointestinal Stromal Tumors

Sergei Boichuk[1], Derek J. Lee[1], Keith R. Mehalek[1], Kathleen R. Makielski[1], Agnieszka Wozniak[3], Danushka S. Seneviratne[1], Nina Korzeniewski[5], Rolando Cuevas[1], Joshua A. Parry[1], Matthew F. Brown[1], James Zewe[1], Takahiro Taguchi[6], Shin-Fan Kuan[2], Patrick Schöffski[3], Maria Debiec-Rychter[4], and Anette Duensing[1,2]

Abstract

Most gastrointestinal stromal tumors (GIST) are caused by oncogenic KIT or platelet-derived growth factor receptor activation, and the small molecule kinase inhibitor imatinib mesylate is an effective first-line therapy for metastatic or unresectable GIST. However, complete remissions are rare and most patients ultimately develop resistance, mostly because of secondary mutations in the driver oncogenic kinase. Hence, there is a need for novel treatment options to delay failure of primary treatment and restore tumor control in patients who progress under therapy with targeted agents. Historic data suggest that GISTs do not respond to classical chemotherapy, but systematic unbiased screening has not been performed. In screening a compound library enriched for U.S. Food and Drug Administration (FDA)–approved chemotherapeutic agents (NCI Approved Oncology Drugs Set II), we discovered that GIST cells display high sensitivity to transcriptional inhibitors and topoisomerase II inhibitors. Mechanistically, these compounds exploited the cells' dependency on continuous KIT expression and/or intrinsic DNA damage response defects, explaining their activity in GIST. Mithramycin A, an indirect inhibitor of the SP1 transcription factor, and mitoxantrone, a topoisomerase II inhibitor, exerted significant antitumor effects in mouse xenograft models of human GIST. Moreover, these compounds were active in patient-derived imatinib-resistant primary GIST cells, achieving efficacy at clinically relevant concentrations. Taken together, our findings reveal that GIST cells have an unexpectedly high and specific sensitivity to certain types of FDA-approved chemotherapeutic agents, with immediate implications for encouraging their clinical exploration. *Cancer Res; 74(4); 1200–13. ©2014 AACR.*

Introduction

Gastrointestinal stromal tumors (GIST) are the most common mesenchymal tumors of the gastrointestinal tract and the most common sarcomas in some geographic regions. Most GISTs are caused by activating mutations of the *KIT* or *PDGFRA (platelet-derived growth factor receptor alpha*) receptor tyrosine kinase genes (1–4) and can be effectively treated with the small molecule tyrosine kinase inhibitor (TKI) imatinib mesylate (Gleevec; refs. 1–4). However, complete remissions are rare, and up to 50% of patients with GIST develop resistance during the course of the first 2 years of systemic treatment (5). Because the approved multikinase inhibitors sunitinib malate (Sutent; ref. 6) and regorafenib (Stivarga; ref. 7) offer only limited additional benefit for the majority of patients (8), novel therapeutic options are needed to prolong disease stabilization, achieve symptomatic benefit, and delay the occurrence of therapy resistance. It is known from a number of studies that resistance to kinase inhibitors is mainly caused by secondary mutations of the driver oncogenic kinase (9, 10). Treatment strategies that do not focus on kinase inhibitors may therefore be advantageous, but have remained largely unexplored in GISTs.

It is widely believed that GISTs respond poorly to chemotherapeutic agents commonly used to treat mesenchymal malignancies (5, 11). This notion, however, is mainly based on clinical studies that were carried out before the characterization of the *KIT/PDGFRA* driver mutations in GIST and the introduction of specific diagnostic markers, such as KIT immunohistochemistry. Taking into account that GISTs and

Authors' Affiliations: [1]Cancer Virology Program, University of Pittsburgh Cancer Institute, Hillman Cancer Center; [2]Department of Pathology, University of Pittsburgh School of Medicine, Pittsburgh, Pennsylvania; [3]Laboratory of Experimental Oncology, Department of General Medical Oncology; [4]Department of Human Genetics, University Hospitals Leuven and KU Leuven, Leuven, Belgium; [5]Molecular Urooncology, University of Heidelberg School of Medicine, Heidelberg, Germany; and [6]Department of Anatomy, Kochi Medical School, Nankoku, Kochi, Japan

Note: Supplementary data for this article are available at Cancer Research Online (http://cancerres.aacrjournals.org/).

Current address for S. Boichuk: Department of Pathology, Kazan State Medical University, Kazan, Russia

Corresponding Author: Anette Duensing, University of Pittsburgh Cancer Institute, Hillman Cancer Center, Research Pavilion, Suite 1.8, 5117 Centre Avenue, Pittsburgh, PA 15213. Phone: 412-623-5870; Fax: 412-623-7715; E-mail: aduensin@pitt.edu

doi: 10.1158/0008-5472.CAN-13-1955

Published OnlineFirst January 2, 2014; DOI: 10.1158/0008-5472.CAN-13-1955

intraabdominal leiomyosarcomas (LMS) are histopathologically very similar, it is possible that earlier clinical trials included gastrointestinal leiomyosarcomas (11), a tumor entity that is known to be highly resistant to chemotherapy. Therefore, a reassessment of the response of GISTs to chemotherapeutic agents is warranted. Additional support for this notion stems from the fact that histone H2AX, a component of the DNA damage and repair machinery, has recently been found to play a role in GIST cell viability and apoptosis (12, 13).

In this study, we performed a compound screen of U.S. Food and Drug Administration (FDA)-approved chemotherapeutic agents [National Cancer Institute (NCI) Approved Oncology Drugs Set II; ref. 14] in GIST cell lines. Unexpectedly, GIST cells were highly sensitive to drugs targeting gene transcription or inhibiting topoisomerase II. Two compounds, mithramycin A and mitoxantrone, were chosen for further investigation and proved to be active in both imatinib-sensitive and imatinib-resistant GIST cell lines, patient-derived primary GIST cells, and 2 xenograft mouse models. Mechanistically, our results are explained by cellular dependence on oncogenically activated *KIT*, which is substantially downregulated on the transcriptional level by mithramycin A, as well as high expression levels of topoisomerase II and/or downregulation of topoisomerase I, which sensitize GIST cells to mitoxantrone-induced DNA damage.

Taken together, our results show that unbiased drug screens can identify novel and unexpected drug sensitivities in GISTs caused by the underlying biologic alterations of the tumor (15). This approach will facilitate the development of novel treatment options and biomarkers of response with a goal toward a personalized approach even for patients with TKI-resistant GIST.

Materials and Methods

Cell culture

The imatinib-sensitive human GIST cell lines GIST882 (kindly provided by J.A. Fletcher, Brigham and Women's Hospital, Boston, MA) and GIST-T1 (16) were derived from untreated metastatic GISTs (12, 17). GIST882 cells carry a homozygous mutation in *KIT* exon 13 (K642E; ref. 18), whereas GIST-T1 cells carry a heterozygous *KIT* exon 11 deletion (V560_Y578del; ref. 16). Imatinib-resistant GIST cell lines GIST430, GIST48, and GIST48B (kindly provided by J.A. Fletcher; ref. 19) were grown as previously described (13). These cells were derived from human GISTs that developed clinical resistance to imatinib therapy. GIST430 carries a heterozygous primary *KIT* exon 11 deletion (V560_L576del) and a secondary *KIT* exon 13 point mutation (V654A), whereas GIST48 cells are characterized by a homozygous primary *KIT* exon 11 mutation (V560D) and a secondary *KIT* exon 17 mutation (D820A). GIST48B cells are derived from GIST48 cells, with which they share the *KIT* mutational status, but have no detectable KIT protein expression (19).

Leiomyosarcoma cell lines (SK-UT1, SK-LMS; American Type Culture Collection) and normal human dermal fibroblasts (Lonza) were maintained according to manufacturer's recommendations.

A short-term culture was established from a patient with a clinically imatinib- and sunitinib-refractory GIST that underwent surgery for removal of a progressing lesion at UPMC Presbyterian Hospital (Pittsburgh, PA; Institutional Review Board protocol no. 0509050) as previously described (13).

In vitro apoptosis and proliferation assays

Apoptosis and cell viability studies were performed using Caspase-Glo and CellTiter-Glo luminescence-based assays (Promega; ref. 13). Cells were plated in 96-well flat-bottomed plates (Perkin Elmer), cultured for 24 hours, and then incubated for 48 hours (Caspase-Glo) or 72 hours (CellTiter-Glo) with the respective compounds at indicated concentrations or dimethyl sulfoxide (DMSO)-only solvent control. Luminescence was measured with a BioTek Synergy 2 Luminometer (BioTek). Data were normalized to the DMSO-only control group.

Compound screen and inhibitor treatments

The NCI Approved Oncology Drugs Set II compound library was obtained from the NCI under a material transfer agreement. It contains 89 FDA-approved anticancer drugs dissolved at 10 mmol/L concentration in DMSO. The full list of drugs is available from the NCI (14) and is also shown in Supplementary Table S1. Cells were cultured in 96-well plates and each screen was performed in triplicate at 2 drug concentrations, 1 and 10 μmol/L, to allow for some therapeutic range. Treatment with DMSO, the KIT inhibitors imatinib and sunitinib (both at 1 μmol/L in DMSO) as well as the proteasome inhibitor bortezomib (0.01 μmol/L in DMSO; all from LC Laboratories) was included in each set of experiments (in triplicate) as negative and positive controls, respectively. Cellular viability and apoptosis were assessed by using luminescence-based assays.

Results from the triplicate screens were averaged and normalized to their respective average DMSO control. These results were then combined into a "response score" using the formula $\left(\text{drug-response score} = \frac{(\text{apoptosis})+(1/\text{viability})}{2}\right)$ to reflect the fact that luminescence values for increased apoptosis were >1 and values for decreased cell viability were <1. Hits were defined as having a response score $\geq$2-fold over DMSO-treated cells (i.e., $\geq$2). Very similar results were obtained when a response score greater than the imatinib (in imatinib-sensitive cells) or sunitinib (in imatinib-resistant cells) score was considered as hit.

For follow-up studies, cells were incubated in imatinib (1 μmol/L), mithramycin A (at various concentrations in DMSO as indicated; Sigma), mitoxantrone (at various concentrations in DMSO as indicated; Thermo Fisher Scientific), α-amanitin (1 μg/mL in dH_2O; Sigma), or mock treated with 0.1% DMSO or dH_2O for up to 72 hours as indicated.

Immunologic and cell staining methods

Protein lysates of cells growing as monolayer were prepared as described previously (20). Xenograft specimens were minced on ice in the presence of lysis buffer and homogenized using a Tissue Tearor (BioSpec; ref. 20). Thirty micrograms of protein were loaded on a 4% to 12% Bis-Tris gel (Invitrogen) and blotted onto a nitrocellulose membrane.

Published OnlineFirst January 2, 2014; DOI: 10.1158/0008-5472.CAN-13-1955

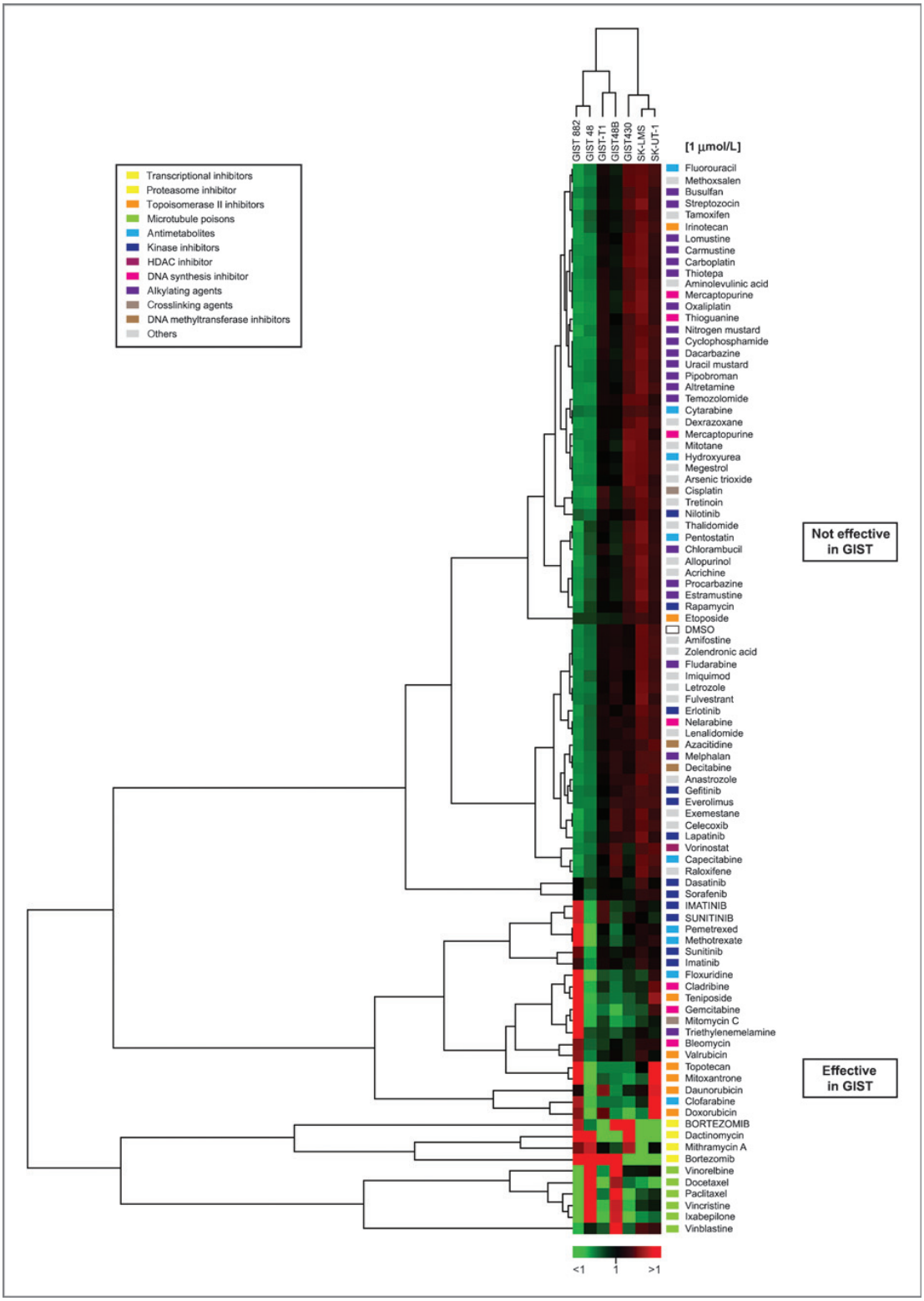

Published OnlineFirst January 2, 2014; DOI: 10.1158/0008-5472.CAN-13-1955

Immunofluorescence analysis for phosphorylated RNA polymerase II and CREB binding protein (CBP) was performed as described previously (12). To assess the cellular localization of pATM S1981, pH2AX S139, MRE11 and 53BP1, Alexa Fluor 488-, or $Cy3^{+}$-conjugated secondary antibodies (Invitrogen and Jackson Immunoresearch, respectively) were used (30 minutes at room temperature in the dark). Cells were analyzed using an Olympus AX70 epifluorescence microscope equipped with a SpotRT digital camera.

Immunohistochemic staining of paraffin-embedded mouse xenograft sections was done as described previously (21).

Primary antibodies used for immunoblotting, immunofluorescence, and immunohistochemistry were the following: actin (Sigma); ATM and pATM S1981 (both Epitomics); pATM S1981 (Rockland); CBP (Santa Cruz A); cyclin A (Novocastra); cleaved caspase-3 (Cell Signaling); H2AX (Bethyl); pH2AX S139 (Millipore); pH3 S10, pKIT Y719 (both Cell Signaling); KIT (DakoCytomation); MRE11 (Novus); PARP (Invitrogen/Zymed Laboratories); RNA polymerase II, pRNA polymerase II S2, and pRNA polymerase II S5 (all Covance); Topoisomerase I (Abcam); Topoisomerase II (Cell Signaling); $p27^{Kip1}$ (BD Biosciences Pharmingen); and 53BP1 (Calbiochem).

Apoptotic cells were visualized using the *In situ* Cell Death Detection Kit (Roche Applied Sciences) according to manufacturer's recommendations (12).

Reverse transcriptase-PCR and quantitative real-time reverse transcriptase-PCR

Reverse transcriptase (RT)-PCR and quantitative real-time RT-PCR (qRT-PCR) were performed as described previously (13, 22). Exon-overlapping, mRNA/cDNA-specific primers were used to amplify *KIT* (forward: 5′-TCATGGTCGGATCACAAAGA-3′, reverse: 5′-AGGGGCTGCTTCCTAAAGAG-3′; Operon) and *β-actin* (forward: 5′-CCAAGGCCAACCGCGAGAAGATGAC-3′, reverse: 5′-AGGGTACATGGTGGTGCCGCCAGAC-3′). *β-Actin* served as reference gene for relative quantification in qRT-PCR experiments.

Comet assay

DNA double-strand breaks (DSB) were detected by using the CometAssay Kit from Trevigen under neutral conditions (23). In brief, cells were treated with DMSO or mitoxantrone for the indicated amount of time. Apoptotic cells were excluded from the assay by removing the supernatant before trypsinising. Cells were then washed in ice-cold PBS, diluted to 75,000 cells/mL, and added to molten LMAgarose. After spotting onto 2-well CometSlides and solidifying, slides were immersed in lysis solution and electrophoresed in chilled TBE buffer (21 V, 10 minutes). Slides were then fixed in 70% ethanol and dried. DNA was labeled with SYBR Green and slides were viewed under a Nikon ECLIPSE 50i epifluorescence microscope (Nikon). Comet tails were analyzed using CometAssay IV v4.2 software (Perceptive Instruments). At least 100 cells were analyzed per sample.

GIST xenograft models

GIST882 or GIST-T1 cells were bilaterally injected in the flank of female adult athymic nude mice (NMRI, nu/nu; Janvier Laboratories; refs. 21 and 24). When tumors were 1 cm in diameter, mice were randomized into groups of 4 animals each for each treatment regimen. Mithramycin A (0.5 mg/kg in PBS) or mitoxantrone (1.5 mg/kg in 0.9% NaCl) was administered intraperitoneally (i.p.) 3 times a week or every 4 days, respectively, for 2 weeks (25, 26). Mice receiving PBS (150 μL, i.p.) were used as negative control. Tumor volume, weight, and general health of the mice were recorded (21). After the mice were sacrificed, tumors were excised and divided for fresh-frozen samples and histopathologic examination. The animal experiment was approved by the Ethics Committee of KU Leuven (Leuven, Belgium).

Histopathologic grading of the response to the compounds was performed (21, 27) and was based on the microscopic amount of necrosis, myxoid degeneration, or fibrosis with grade 1 representing a minimal response (0–10%) and grade 4 representing a maximal response (>90%). Apoptotic and mitotic cells were visualized by immunohistochemical staining for cleaved caspase-3 and phosphorylated histone H3 S10, respectively (21). The number of positive cells was counted per 10 high power fields (HPF) at 400-fold magnification.

Statistics

Statistical significance was assessed using the Student *t* test for independent samples and the Mann–Whitney *U* test for not normally distributed samples (VassarStats, http://vassarstats.net). *P* values ≤ 0.05 were considered significant. Unsupervised hierarchical clustering analysis was performed using Cluster 3.0 (28) and visualized using MapleTree (http://www.eisenlab.org/eisen).

Results

A compound screen identifies inhibitors of transcription and of topoisomerase II as active agents against GIST cells

To determine the sensitivity of GIST cells to chemotherapeutic agents, we performed a screen using the NCI/NIH Approved Oncology Drugs Set II (14), which consists of 89 FDA-approved compounds (Supplementary Table S1). Two imatinib-sensitive (GIST882 and GIST-T1) and 3 imatinib-resistant (GIST430, GIST48, and GIST48B) human GIST cell lines were tested. Because it is conceivable that historically GISTs were frequently misclassified as

Figure 1. Enhanced chemosensitivity distinguishes GIST from leiomyosarcoma cells. Two-way unsupervised hierarchical clustering of the response scores of 5 GIST and 2 leiomyosarcomas cell lines to 89 FDA-approved anticancer drugs (NCI Approved Oncology Drugs Set II) at a concentration of 1 μmol/L (mean values of triplicate experiments). Clustering was done using Cluster 3.0 (28). The height of the "tree" indicates the quality of the correlation. Each row represents a tested drug; cell lines are arranged in columns. Drugs are color-coded according to their mechanism of action (also see Supplementary Table S1). Response scores of >1 (effective drugs) are shown in red, response scores of <1 (ineffective drugs) are shown in green. Note the clustering according to cell type as well as compound class within the group of effective compounds for GIST cells. Control compounds are shown in capital letters.

Published OnlineFirst January 2, 2014; DOI: 10.1158/0008-5472.CAN-13-1955

abdominal leiomyosarcoma, 2 leiomyosarcomas cell lines (SK-LMS and SK-UT-1) were analyzed in direct comparison.

A total of 37 compounds were identified that had antitumor activity in at least 1 GIST cell line for at least one of the concentrations tested (Supplementary Table S1). Many of the active compounds had response scores that were substantially higher than the response scores of imatinib or sunitinib. Importantly, a 2-way unsupervised hierarchical clustering analysis separated GIST and leiomyosarcoma cells (Fig. 1). Although 1 GIST cell line (GIST430) clustered close to the SK-LMS and SK-UT-1 cells, this unbiased analysis underscores a trend toward the different drug sensitivities of these 2 tumor entities. Compounds that showed activity in GIST cells clustered according to their mode of action (Fig. 1). The most effective compound classes were transcriptional inhibitors and inhibitors of topoisomerase II, especially those with intercalating properties.

The most effective compound in our screen was the proteasome inhibitor bortezomib with strong activity in all GIST cell lines tested. This confirms our previous study that had identified bortezomib as an effective compound against GIST cells (13). The compounds that ranked second and third in antineoplastic efficacy were the transcriptional inhibitors mithramycin A and dactinomycin, which showed activity in all GIST lines tested (Fig. 1 and Supplementary Table S1). Remarkably, bortezomib has previously been shown to function in part through blocking ongoing gene transcription in GIST (13) and these 3 compounds, mithramycin A, dactinomycin, and bortezomib, were found to cluster (Fig. 1).

Additional agents with high antitumor activity in GIST cells were topoisomerase II inhibitors, especially those with an additional intercalating property, such as mitoxantrone, daunorubicin, doxorubicin, and valrubicin (Fig. 1 and Supplementary Table S1). GIST cells were resistant to most alkylating agents as well as estrogen receptor modulators, aromatase inhibitors, photo-activated drugs, and immunomodulatory agents (Supplementary Table S1). Microtubule poisons showed some sensitivity in GIST48 and its derivative GIST48B (Supplementary Table S1) but not in other GIST cell lines.

Taken together, our screen of a library of FDA-approved compounds in GIST cells showed significant antitumor activity of 2 main drug classes, inhibitors of gene transcription and inhibitors of topoisomerase II.

Mithramycin A and mitoxantrone are effective inducers of apoptosis and cell-cycle arrest in imatinib-sensitive and imatinib-resistant GIST cells

Having identified inhibitors of gene transcription and topoisomerase II inhibitors as 2 main drug classes with activity in GIST cells, we selected one compound of each class, mithramycin A and mitoxantrone, for further validation. These studies were carried out in 1 imatinib-sensitive (GIST882) and 1 imatinib-resistant (GIST430) cell line.

Treatment of GIST882 and GIST430 cells with increasing concentrations of mithramycin A (0.001–10 μmol/L) induced a statistically significant proapoptotic and growth-suppressive effect that was seen in both cell lines beginning at concentrations of 0.1 μmol/L (Fig. 2A and Supplementary Fig. S1A). Likewise, concentration-dependent cleavage of PARP and caspase-3 was detected by immunoblotting in both cell lines starting at 0.1 μmol/L, indicating the onset of apoptosis (Supplementary Fig. S1B). At the same time, expression of the S-phase marker cyclin A decreased in a concentration-dependent manner. Based on these results, the lowest effective concentration of mithramycin A was defined as 0.1 μmol/L and was used in all further experiments.

For mitoxantrone, a statistically significant increase in apoptosis and reduction of cell viability was seen starting at 0.1 μmol/L in GIST882 (Fig. 2B), whereas these effects were only seen at concentrations of 1.0 and 10.0 μmol/L in GIST430 (Fig. 2B). A terminal deoxynucleotidyl transferase–mediated dUTP nick end labeling (TUNEL) assay confirmed the higher sensitivity of GIST882 to mitoxantrone when compared with GIST430 (Supplementary Fig. S2A). Immunoblot analysis showed strong apoptosis-associated PARP and caspase-3 cleavage after 1.0 μmol/L mitoxantrone in GIST882, whereas the effect was less pronounced in GIST430 at these concentrations (Supplementary Fig. S2B). Protein expression of the S-phase marker cyclin A was completely lost at 10 μmol/L in both GIST882 and GIST430 (Supplementary Fig. S2B). Based on these results, the minimum effective concentrations for mitoxantrone was defined as 1 μmol/L for GIST882 and 5 μmol/L in GIST430.

It is important to note that the minimal effective concentrations defined in our study (0.1 μmol/L mithramycin A and 1 to 5 μmol/L mitoxantrone) are clinically achievable in humans. Plasma levels of mithramycin have been reported to reach peak concentrations of 0.30 to 0.35 μmol/L after a 2-hour continuous infusion of the standard dose of 25 μg/kg (29). The standard dose of mitoxantrone in humans (10–14 mg/m^2) produces peak plasma concentrations in the range of 1.0 μmol/L (30–32), but high-dose regimens using up to 80 mg/m^2 have been tested extensively and have been deemed safe (33). In summary, these results demonstrate that mithramycin A and mitoxantrone exert their antineoplastic activities in GIST cells at concentrations that are relevant for the clinic and can be achieved in the sera of patients with cancer (32, 34).

The response to mithramycin A and mitoxantrone is time dependent

To ascertain the time dependency of the effects of mithramycin A and mitoxantrone in GIST cells, we treated GIST882 and GIST430 cells at the minimal effective concentrations for 1 to 72 hours (Fig. 2C–E).

Mithramycin A caused an apoptotic response starting after 24 hours in GIST882 and GIST430 cells (Fig. 2C and D). Levels of the S-phase marker cyclin A decreased in parallel with apoptosis induction (Fig. 2C).

Mitoxantrone induced a more rapid onset of apoptosis in GIST882 starting after 8 hours of treatment (Fig. 2E). In GIST430 cells, an apoptotic response was detected after 24 hours (Fig. 2E). There was a very strong apoptotic effect in GIST430 after 72 hours as reflected by nearly complete PARP and caspase-3 degradation (Fig. 2E and F). Mitoxantrone also

Published OnlineFirst January 2, 2014; DOI: 10.1158/0008-5472.CAN-13-1955

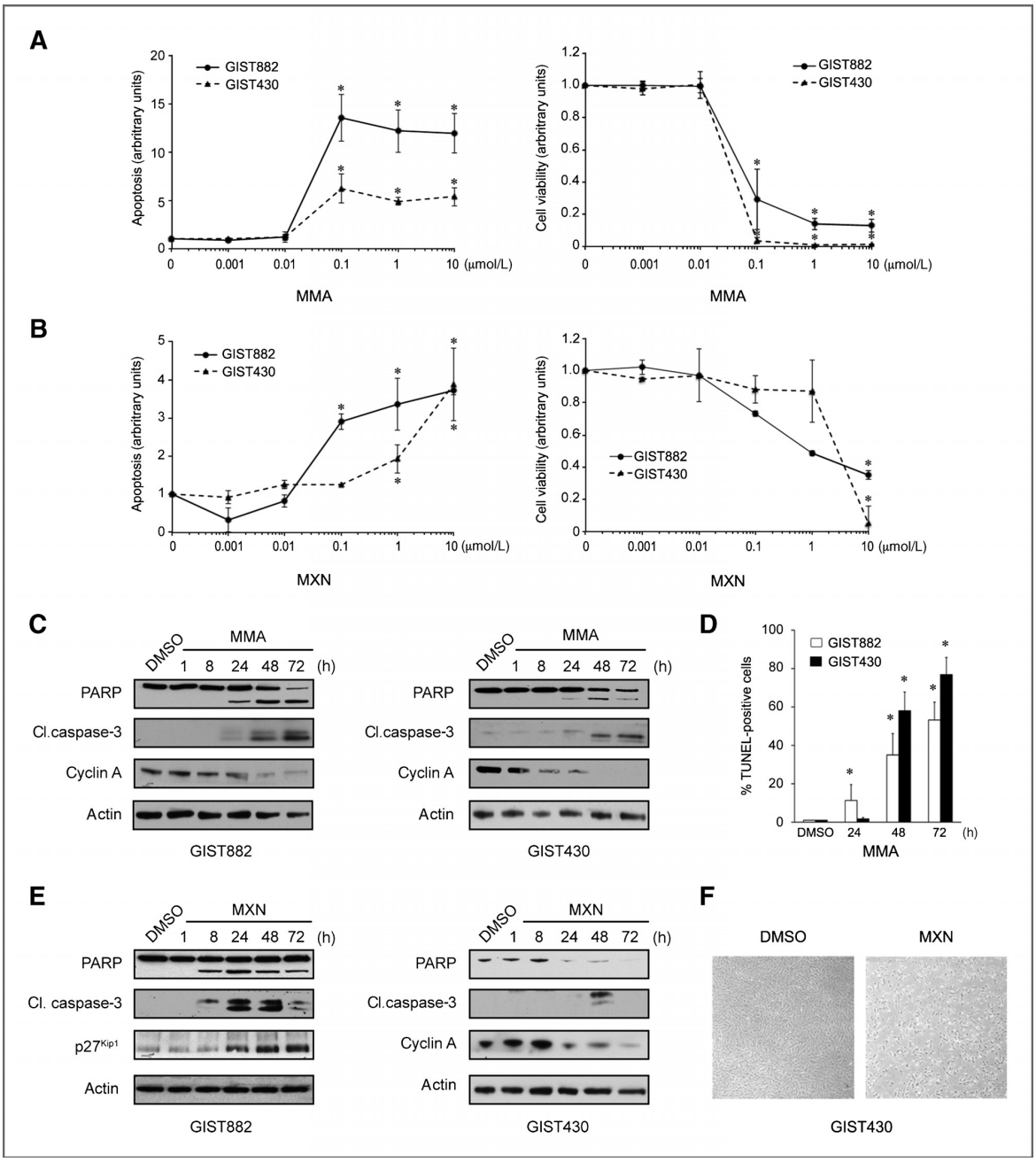

Figure 2. The transcriptional inhibitor mithramycin A (MMA) and the topoisomerase II inhibitor mitoxantrone (MXN) effectively induce time-dependent GIST cell apoptosis and cell-cycle arrest. A and B, dose-dependent effect of MMA (A) and MXN (B) on apoptosis (left) and cell viability (right) of GIST882 and GIST430 cells as measured by luminescence-based assays (mean + SE). *, $P \leq 0.05$ in comparison with control. C and D, immunoblot analysis (C) for markers of apoptosis and cell-cycle regulation and TUNEL assay (D) in GIST cells after treatment with DMSO or 0.1 μmol/L MMA for the indicated times. E, immunoblot analysis for markers of apoptosis and cell-cycle regulation in GIST cells after treatment with DMSO or MXN at indicated concentrations for 72 hours or with MXN at the indicated times. F, brightfield image of GIST430 cells treated with DMSO or MXN (5 μmol/L) for 72 hours.

led to an exit of the cell division cycle as shown by increased levels of $p27^{Kip1}$ in GIST882 and a decrease in cyclin A in GIST430 (Fig. 2E).

Taken together, our results show differences in the timing of apoptosis induction and growth suppression between mithramycin A (24 hours in GIST882 and GIST430) and mitoxantrone

Published OnlineFirst January 2, 2014; DOI: 10.1158/0008-5472.CAN-13-1955

(8 hours in GIST882 and 24 hours in GIST430) that may reflect distinct mechanisms of action.

Mithramycin A leads to loss of KIT expression, transcriptional inhibition, and activation of a DNA damage response

We next sought to confirm the mechanism of action of the proapoptotic and growth inhibitory activities of mithramycin A and mitoxantrone in GIST cells.

Mithramycin A has DNA-binding properties that lead to an inhibition of gene transcription mediated by SP1 (35, 36), one of the major transcriptional activators of the *KIT* gene (37). Because expression of oncogenically activated KIT is a tumor-specific, crucial driver of GIST pathogenesis and survival, GIST cells are critically dependent on the expression of mutant KIT (12, 13, 38). We therefore tested first whether mithramycin A treatment causes a downregulation of *KIT* transcription. We found a substantial downregulation of *KIT* mRNA expression levels in mithramycin A–treated GIST cells by RT-PCR and qRT-PCR (Fig. 3A). The effect was comparable with cells treated with the RNA polymerase (pol) II inhibitor α-amanitin (Fig. 3A). Importantly, reduced *KIT* mRNA levels after mithramycin A treatment led to a complete abrogation of KIT protein expression and activation starting at 8 hours after treatment in both GIST882 and GIST430 cells (Fig. 3B). The effect on KIT transcription and expression was specific for mithramycin A, because it was not seen in cells treated with mitoxantrone (Fig. 3A).

To further characterize the effects of mithramycin A on ongoing gene transcription, we determined expression and activation of the core transcriptional machinery. Mithramycin A led to a loss of active RNA pol II from chromatin both in its initiating form (S5 phosphorylation of the RNA pol II carboxyl-terminal repeat domain, CTD) and elongating form (S2 phosphorylation of the CTD; Fig. 3C; ref. 39). Immunoblotting demonstrated a loss of pRNA pol II S5 and S2 as well as total RNA pol II in a time-dependent manner (Fig. 3D), a finding that has been described to occur during prolonged transcriptional stalling (40). In addition, mithramycin A induced a redistribution of the transcriptional coactivator CREB-binding protein (CBP) into a coarsely speckled pattern in the nucleus (foci) that is associated with inactive gene transcription (Fig. 3E; ref. 39). These results underscore that reduced *KIT* mRNA levels after mithramycin A may be the result of 2 mechanisms: inhibition of SP1-mediated transcription and a more general attenuation of ongoing gene transcription. Furthermore, it is likely that both processes affect additional vital gene products thereby adding to the effectiveness of the drug.

It has been shown that a prolonged transcriptional block can cause DNA damage (41). In addition, direct binding of mithramycin A to DNA can potentially lead to DNA replication fork stalling (35, 36). We therefore asked whether mithramycin A treatment would also induce a measurable DNA damage response. We found that mithramycin A led to an increase of phosphorylated ATM S1981 after approximately 24 hours (Fig. 3F). This DNA damage response effect was somewhat delayed when compared with the measurable onset of transcriptional inhibition (approximately 8 hours), suggesting that the induction of DNA damage is a secondary effect that may be cell-cycle dependent. In line with this notion, a proportion of cells is still expressing S-phase markers at 24 hours after mithramycin A treatment (Fig. 2C). The fact that pATM S1981 and pH2AX S139 nuclear foci that colocalized with MRE11 and 53BP1, respectively, were detected (Fig. 3G) underscored the induction of a DNA DSB response.

Taken together, mithramycin A has a dual mechanism of targeting GIST cells for apoptosis by inhibiting ongoing gene transcription and inducing DNA damage.

Mitoxantrone induces a rapid DNA DSB response in GIST cells

As expected, based on its known mode of action (42), mitoxantrone rapidly induced phosphorylation of the DNA DSB response protein ATM at S1981 in both GIST882 and GIST430 cells (1 hour; Fig. 4A). In addition, mitoxantrone led to the formation of DSB-associated nuclear pH2AX S139 foci in GIST882 and GIST430 (Fig. 4B).

To prove that the rapid ATM phosphorylation induced by mitoxantrone indeed represents the induction of DNA DSBs, a Comet assay was performed. Mitoxantrone treatment caused DNA fragmentation as evidenced by so-called Comet tails in GIST882 and GIST430 cells (Fig. 4C). This effect was quantified by analyzing Comet tail intensity and tail moment, both of which were significantly altered after mitoxantrone treatment, indicating DNA breakage (Fig. 4C, right).

Topoisomerase expression levels have been shown to correlate with sensitivity to topoisomerase II inhibitors, including mitoxantrone (43). In particular, low expression levels of topoisomerase II have been reported to confer drug resistance, whereas high levels can sensitize to topoisomerase II inhibition (44). Moreover, low levels of topoisomerase I were found to correlate with increased sensitivity to topoisomerase II inhibitors (44). We hence analyzed topoisomerase I and II protein expression in GIST882 and GIST430 by immunoblotting (Fig. 4D). We found a markedly decreased expression of topoisomerase I in GIST882 cells in comparison with controls as well as increased levels of topoisomerase II expression in GIST430, which can explain the sensitivity of these cells to mitoxantrone. However, this finding does not readily explain the lower sensitivity of GIST430 to the drug when compared with GIST882.

To further explore this perplexing finding, we decided to further dissect the DNA DSB response in GIST430 cells in comparison with GIST882 cells after mitoxantrone treatment. As shown by immunofluorescence microscopy, GIST430 cells had a severe defect in the proper formation of DNA damage–associated nuclear foci that contain pATM S1981 and 53BP1 (Fig. 4E). This finding correlated with the inability of GIST430 cells to maintain ATM phosphorylation (Fig. 4A) despite the presence of broken DNA (Fig. 4C).

Taken together, our results show that mitoxantrone induces DNA breakage in both GIST882 and GIST430 cells. Although GIST882 cells mount a rapid DNA damage response and start to undergo apoptosis after 8 hours of drug treatment, GIST430 show a defective DNA damage response and a delayed but massive apoptosis induction (Fig. 2F). Apoptosis in these cells

Published OnlineFirst January 2, 2014; DOI: 10.1158/0008-5472.CAN-13-1955

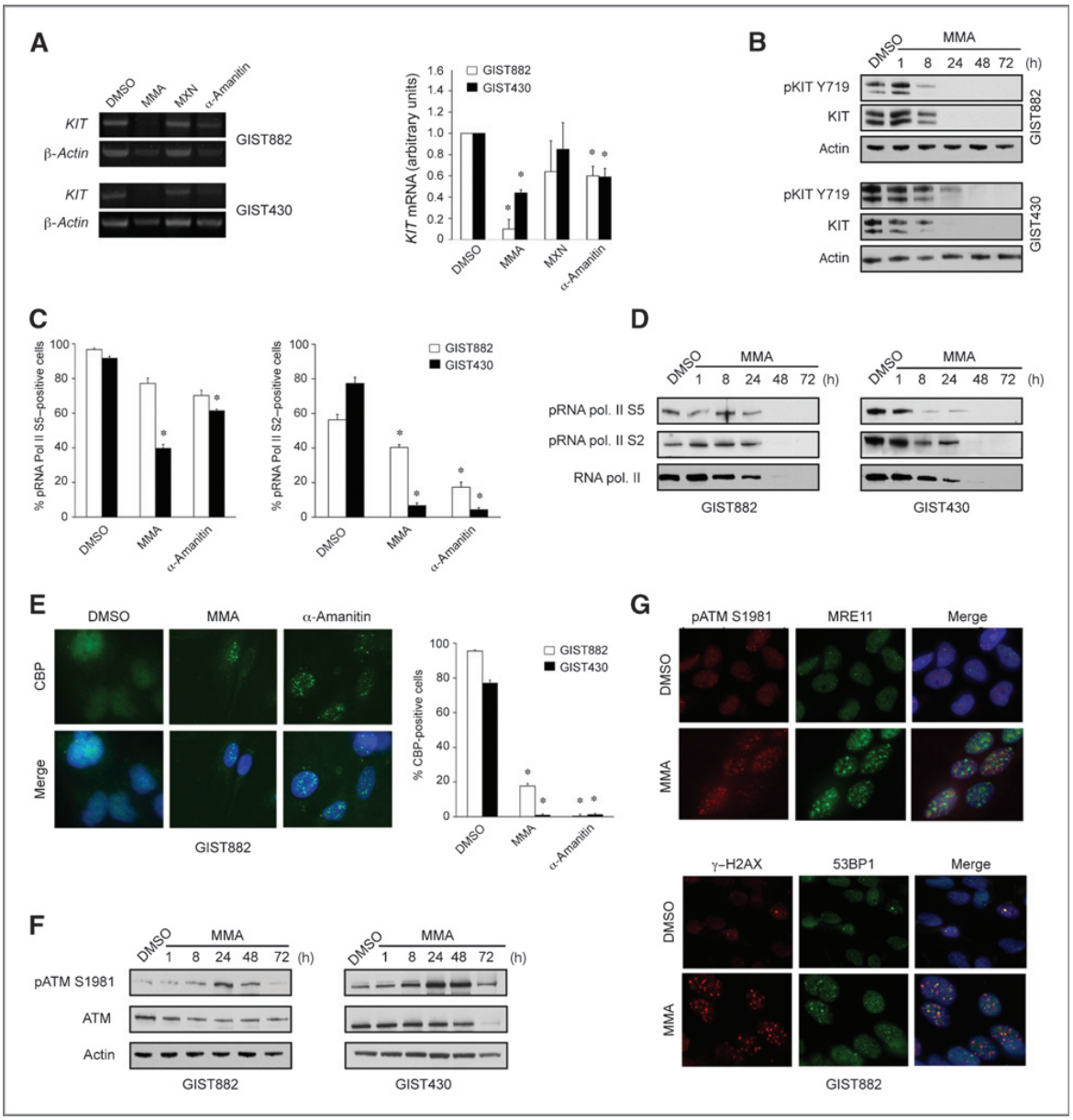

Figure 3. MMA stimulates GIST cell death by transcriptional inhibition and induction of a cellular DNA damage response. A, RT-PCR (left) and quantitative RT-PCR (qRT-PCR; right) amplification of *KIT* mRNA in GIST cells after treatment with DMSO, MMA (0.1 μmol/L), MXN (1 μmol/L, GIST882; 5 μmol/L, GIST430), or α-amanitin (1 μg/mL) for 48 hours. Amplification of *β-actin* mRNA is shown to demonstrate equal loading (RT-PCR, left). qRT-PCR values are normalized against *β-actin* mRNA values. Columns, mean + SE; *, $P \leq 0.05$ in comparison with DMSO controls. B, immunoblot analysis of GIST cells treated with DMSO or MMA for the indicated times and probed for phosphorylated KIT (Y719) and KIT. Actin is shown as a loading control. C, quantification of the percentage of GIST882 and GIST430 cells showing a normal, fine-speckled nuclear staining pattern for pRNA polymerase (pol) II (S5, left graph) or pRNA pol II (S2, right graph) as examined by immunofluorescence microscopy after treatment with DMSO, MMA, or α-amanitin for 48 hours. Columns, mean + SE; *, $P \leq 0.05$ when compared with controls. D, immunoblot analysis of GIST882 and GIST430 cells treated with DMSO or MMA for up to 72 hours and probed for pRNA pol II (S5), pRNA II pol (S2), and total RNA pol II. For loading control, see actin stains in B. E, immunofluorescence microscopic analysis of GIST882 cells treated with DMSO, MMA, or α-amanitin for 48 hours and stained for CREB binding protein (CBP, left). Nuclei were stained with 4′,6-diamidino-2-phenylindole (DAPI; blue). Note the diffuse nuclear staining in DMSO controls and the redistribution into nuclear foci in the treated cells, indicating transcriptional inactivation. Quantification of the percentage of GIST882 or GIST430 cells showing a normal nuclear staining pattern for CBP (right) after treatment with DMSO, MMA, or α-amanitin for 48 hours. Columns, mean + SE; *, $P \leq 0.05$ when compared with controls. F, immunoblot analysis of GIST882 and GIST430 cells treated with DMSO or MMA for up to 72 hours and probed for pATM S1981 and total ATM. Actin is shown as a loading control. G, immunofluorescence microscopic analysis of GIST882 for DNA damage response–associated nuclear foci (top, pATM S1981 and MRE11; bottom, γ-H2AX and 53BP1) after MMA treatment for 48 hours. Nuclei in stained with DAPI (blue), ×100 magnification.

Published OnlineFirst January 2, 2014; DOI: 10.1158/0008-5472.CAN-13-1955

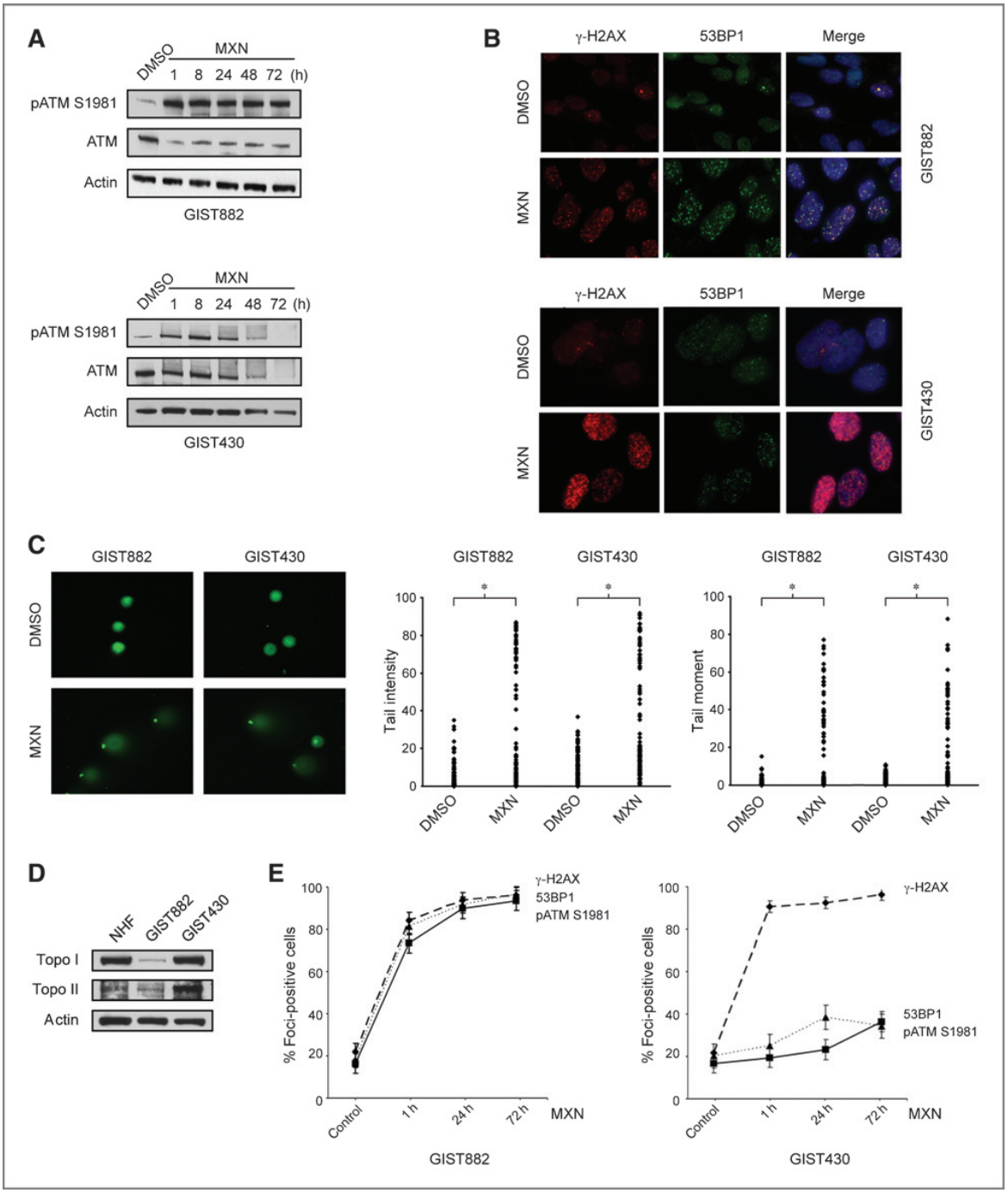

Figure 4. Response of GIST cells to MXN involves topoisomerase expression and robustness of the cellular DNA damage machinery. A, immunoblot analysis of GIST882 and GIST430 cells treated with DMSO or MXN (1 μmol/L, GIST882; 5 μmol/L, GIST430) for up to 72 hours and probed for pATM S1981 and total ATM. Actin is shown as a loading control. B, immunofluorescence microscopic analysis of GIST882 (top) and GIST430 (bottom) cells for γ-H2AX and 53BP1 after MXN treatment (1 μmol/L, GIST882; 5 μmol/L, GIST430) for 48 hours. Nuclei in stained with DAPI (blue), ×100 magnification. C, detection of DNA DSBs in a Comet assay performed under neutral conditions after treating GIST882 and GIST430 cells with DMSO (24 hours) or MXN (72 hours; GIST882, 1 μmol/L; GIST430, 5 μmol/L; left). Quantification of tail intensity (% of DNA in Comet tail, left graph) and tail moment (right graph). *, $P < 0.0001$ compared with control (Mann–Whitney *U* test). D, immunoblot analysis of topoisomerase I and topoisomerase II (α isoform) expression levels in GIST882 and GIST430 cells in comparison with normal human fibroblasts (NHF). Actin is shown as a loading control. E, quantification of the kinetics of the appearance of γ-H2AX (dashed line), pATM S1981 (solid line), and 53BP1 (punctate line) nuclear foci in GIST882 and GIST430 cells as assessed by immunofluorescence staining after MXN treatment (GIST882, 1 μmol/L; GIST430, 5 μmol/L) at the indicated time points. Cells treated with DMSO were used as a negative control.

Published OnlineFirst January 2, 2014; DOI: 10.1158/0008-5472.CAN-13-1955

is therefore most likely not because of a coordinated DNA damage-induced activation of proapoptotic pathways (as in GIST882), but rather because of a mechanism that involves transition into a different cell-cycle stage, such as mitotic catastrophe (45).

Inhibitors of transcription and of topoisomerase II are effective in patient-derived imatinib and sunitinib double-resistant GIST cells

Having shown that mithramycin A and mitoxantrone have significant activity in permanent imatinib-sensitive and imatinib-resistant GIST cell lines, we aimed to corroborate our results in patient-derived primary GIST cells. As expected, treatment of clinically imatinib- and sunitinib-resistant primary GIST cells with imatinib or sunitinib had no effect on tumor cell viability (Supplementary Fig. S3A). Of 5 compounds tested in these primary cells, only treatment with mithramycin A led to significant caspase-3 cleavage and almost complete degradation of PARP, indicating a strong apoptotic response. Mithramycin A and treatment with the topoisomerase II inhibitor etoposide (5 μmol/L) led to a substantial reduction of cell proliferation as measured by decreased levels of cyclin A and an increase in $p27^{Kip1}$ levels. Of note, the proteasome inhibitor bortezomib also induced apoptosis as detected by a PARP cleavage fragment in these cells.

Mithramycin A and mitoxantrone are effective in GIST xenograft models

Finally, we tested the antitumor activity of mithramycin A and mitoxantrone *in vivo* using GIST xenograft models (21, 24).

Both mithramycin A and mitoxantrone had a significant effect on apoptosis induction and cell-cycle inhibition as detected by immunoblotting of proteins extracted from excised GIST882 xenografts (Supplementary Fig. S3B). Both compounds also induced major histopathologic changes in this model (Fig. 5A). Mithramycin A treatment led to a dramatic response according to a previously defined histopathologic response score (21, 27). Importantly, these morphologic findings, which included a central necrosis surrounded by a zone of myxoid degeneration, phenocopy the *in vivo* response to imatinib treatment (21). The histopathologic response to mitoxantrone was remarkably different and resulted in extensive intratumoral hemorrhage and single cell death (Fig. 5A).

Both mithramycin A or mitoxantrone treatment caused a significantly increased intratumoral apoptosis as detected by immunohistochemical staining for cleaved caspase-3 (464 and 327 apoptotic cells per 10 HPF in mithramycin A- and mitoxantone-treated cells, respectively, compared with 66 apoptotic cells/10 HPF in placebo-treated controls; $P < 0.0003$ and <0.0001, respectively; Fig. 5B). Furthermore, treatment with mithramycin A or mitoxantrone significantly reduced the

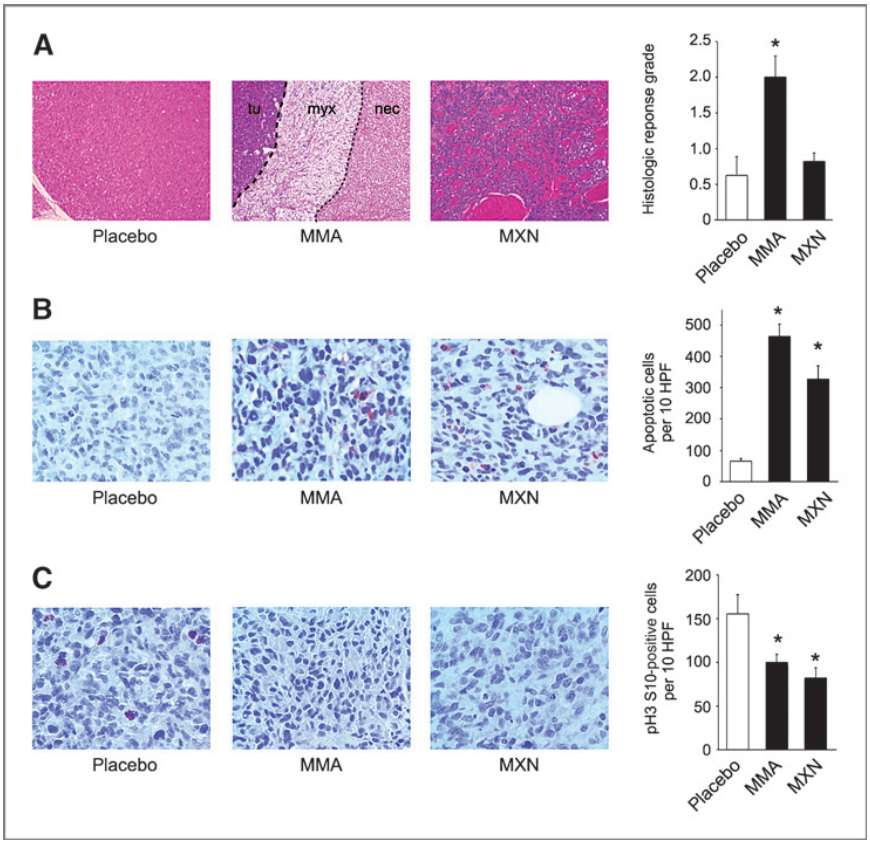

Figure 5. *In vivo* activity of MMA and MXN in a murine GIST xenograft model. A, histopathologic response of GIST xenografts to treatment with MMA and MXN in comparison with placebo (hematoxylin and eosin, ×10 magnification; top). Data shown in graph represent the average of at least 8 tumors per group. Columns, mean + SE; *, $P \leq 0.05$. Dashed lines in MMA-treated histographs separate viable tumor (tu), necrosis (nec), and myxoid degeneration (myx). B and C, immunohistochemical staining for cleaved caspase-3 (B) or phosphorylated histone H3 S10 (C) in GIST xenografts treated with MMA or MXN in comparison with placebo (magnification, ×40; left). Quantification of apoptotic (B) or mitotic cells (C; brown staining, respectively) per 10 HPF (right) represents the average of at least 8 tumors per group. Columns, mean + SE; *, $P \leq 0.05$.

Published OnlineFirst January 2, 2014; DOI: 10.1158/0008-5472.CAN-13-1955

number of mitotic cells as measured by positivity for phosphorylated histone H3 S10 (from 155/10 HFP in controls to 100 and 82/10 HPF in mithramycin A- and mitoxantrone-treated cells, respectively; $P < 0.023$ and <0.009; Fig. 5C). These results were confirmed in a second xenograft model (GIST-T1; ref. 24), in which mithramycin A and mitoxantrone also significantly reduced the number of histone H3 S10-positive mitotic cells (from 381/10 HPF in controls to 158 and 132/10 HPF in mithramycin A- and mitoxantrone-treated cells, respectively; both $P < 0.0001$; Supplementary Fig. S3C).

Although there was no objective reduction in tumor size after mithramycin A or mitoxantrone, the growth of the xenografts was attenuated when compared with control-treated animals (Supplementary Fig. S3D and S3E). Importantly however, mithramycin A or mitoxantrone treatments did lead to significant intratumoral changes as described above, thereby clearly demonstrating the effectiveness of the treatment (Fig. 5A). It is of note that such changes would not necessarily result in a reduction of tumor size, which is in line with the typical clinical response to imatinib as well as imatinib-treated xenografts (21).

Taken together, both mithramycin A and mitoxantrone treatment showed significant antitumor activity *in vivo* using GIST xenograft mouse models.

Discussion

Imatinib mesylate (Gleevec) has revolutionized treatment and prognosis of patients with GIST (2). Nevertheless, the majority of patients develops resistance to imatinib as well as the only FDA-approved second- and third-line therapies, sunitinib malate (Sutent) and regorafenib (Stivarga), over time (5, 7, 8). Novel therapeutic strategies are hence urgently needed.

To effectively identify active compounds and to be able to rapidly move candidate drugs into the clinic, we screened compounds of the NCI Approved Oncology Drugs Set II (14) for their antitumor activity in a panel of GIST cell lines. We identified a number of highly active compounds that mostly belonged to 2 distinct drug classes, inhibitors of gene transcription and topoisomerase II inhibitors.

The notion that GISTs are not sensitive to conventional chemotherapy originates from earlier clinical trials (11) that may have been biased by the inadvertent inclusion of histopathologically similar, but highly chemoresistant tumors, such as abdominal leiomyosarcomas. As a result, the actual response rate of GISTs to chemotherapy may have been underestimated. Neither mithramycin A nor mitoxantrone, the 2 compounds that were chosen for further follow-up in our study because of their high activity in GIST cells *in vitro* and *in vivo*, have systematically been tested for systemic treatment of GIST.

Nevertheless, it is of note that mitoxantrone yielded favorable results when used intraperitoneally to prevent local recurrence of abdominal sarcomas (46). It is worth mentioning, however, that this study did not record the clinical effect of the treatment by histopathologic tumor entity. In addition, data were obtained during the early 1990s, when an unequivocal identification of GISTs was difficult because of the lack of reliable diagnostic markers. Yet, there is more recent evidence for the clinical activity of topoisomerase II inhibitors in GIST. When treated with doxorubicin in combination with imatinib, 36% of imatinib-resistant patients were reported to have had clinical benefit, especially a subgroup of patients without detectable *KIT*/*PDGFRA* mutations (47). Conversely, our compound screen highlighted a remarkable resistance of GIST cells to alkylating agents. These results are supported by clinical findings from a study that tested the alkylator temozolomide in patients with GIST and found a very low response rate to this treatment (48). Taken together, our systematic approach to revisiting chemotherapeutic agents for GIST therapy resulted in the identification of highly effective but also inactive compounds that, to a certain extent, are reflected by anecdotal clinical evidence. Interestingly, a recent study reported activity of another FDA-approved compound, auranofin, an oral, gold-containing agent used to treat rheumatoid arthritis, in GIST cells (49).

Mithramycin A has recently gained attention in the treatment of Ewing sarcoma (25). This compound was the top hit in a 50,000 compound screen to identify inhibitors of the EWS-FLI1 transcription factor, the hallmark of the Ewing sarcoma family of tumors (25). Similar to the results presented here, the minimally active concentration of mithramycin A was relatively low (0.1 μmol/L), an activated DNA damage response was detected, and the compound was effective in a xenograft model. A study testing the clinical activity of mithramycin in patients with Ewing sarcoma has been initiated and is currently recruiting patients (NCT01610570; ref. 50). Thus, mithramycin A seems to be particularly effective in sarcomas and other malignancies, including GIST, that critically depend on ongoing gene transcription.

Mithramycin A competitively binds to GC-rich promoter regions thereby replacing the transcription factor SP1 (35, 36). Through this mechanism, mithramycin A inhibits the transcription of many SP1-regulated genes such as *MYC* and *SRC* (51, 52). Interestingly, SP1 is also a major transcriptional activator of the *KIT* gene (37) and its inhibition in GIST cells by mithramycin A thus led to a substantial decrease of *KIT* mRNA and protein expression and hence reduced KIT activation. Because of the essential role that expression of oncogenic *KIT* plays for GIST cell survival, these changes provide a compelling mechanistic explanation for the induction of apoptosis in these cells. Moreover, inhibition of SP1-mediated transcription of SRC family kinase (SFK) expression could have an additive effect of mithramycin A treatment in GIST as SFKs have been shown to play important roles in GIST cell biology (52, 53). Because of its role as inhibitor of SP1, it has been postulated that mithramycin A leads to a relatively gene-specific downregulation of transcription. However, in our study we detected displacement and loss of active RNA polymerase II and the transcriptional coactivator CBP from chromatin after treatment with mithramycin A, indicating a more global inhibition of cellular transcription that may affect additional vital gene products. In addition to the direct effect on gene transcription, we could show that mithramycin A triggered a DNA damage response in GISTs, as indicated by the formation of DNA damage-associated nuclear foci. This

Published OnlineFirst January 2, 2014; DOI: 10.1158/0008-5472.CAN-13-1955

response was delayed when compared with DNA DSB inducers (such as mitoxantrone) as well as the onset of downregulation of KIT expression by mithramycin A, indicating that it is a secondary effect that occurs after prolonged transcriptional stalling and/or when a stalled DNA replication fork at the site of mithramycin A binding to DNA is converted to a DSB. Taken together, mithramycin A may be specifically effective in GIST through several mechanisms: competitive displacement of SP1 from the KIT promoter leading to rapid downregulation of KIT expression and activation, transcriptional downregulation of cellular oncoproteins other than KIT, such as SRC, global inhibition of cellular transcription, and the induction of a DNA DSB response. All mechanisms are independent of direct KIT kinase inhibition and therefore irrespective of a secondary mutation as mechanism of resistance meaning that mithramycin A is effective in imatinib-sensitive and imatinib-resistant GIST.

Topoisomerase II inhibitors, such as mitoxantrone, are known to induce DNA breakage by stabilizing a usually transient DSB that is catalyzed by topoisomerase II to relieve conformational and topologic changes in DNA during replication. Mitoxantrone has been shown to rapidly induce these breaks *in vitro* (54), a finding that we confirmed in GIST cells by showing a rapid activation of ATM as well as by the detection of fragmented DNA in a Comet assay. Although protein expression levels of topoisomerase I (low in GIST882) and II (high in GIST430) could explain the sensitivity of GIST882 cells, they failed to explain the lower sensitivity and delayed apoptosis induction in GIST430 cells. However, we discovered that GIST430 cells have a defective DNA damage response and fail to assemble proper DNA damage foci and maintain ATM activation despite DNA damage. It is hence possible that GIST882 cells rapidly undergo apoptosis in response to DNA damage by activating proapoptotic signaling pathways. In contrast, GIST430 cells seem to contain damaged DNA without a proper DNA damage response, which could trigger alternative forms of cell death that require a longer time interval, such as mitotic catastrophe, where cells have to move to a different cell-cycle stage before they undergo cell death.

One possibility of achieving an enhanced therapeutic effect is to use drugs in combination. In an attempt to do so, we have tested several combinations of imatinib with either mithramycin A or mitoxantrone in both imatinib-sensitive and imatinib-resistant GIST cells *in vitro*. These preliminary experiments did not show evidence for synergy (data not shown). Interestingly, similar results were obtained in a study by Lee and colleagues when simultaneously treating breast cancer cells with the EGFR inhibitor erlotinib and the topoisomerase II inhibitor doxorubicin (55). Time-staggered, sequential treatments, however, significantly sensitized these cells to undergo apoptosis, presumably because of extensive network rewiring. Addressing this question in GIST cells will be subject of future studies.

In summary, we have shown that an unbiased compound screen can identify novel drug sensitivities in GIST that can be exploited clinically. Importantly, we were able to link drug activities to intrinsic molecular requirements and defects, such as continued *KIT* transcription, differences in topoisomerase expression, or defects in the cellular DNA damage response. Our study provides a framework for the future development of mono- or combination therapies and biomarkers predicting the individual response of patients with GIST with an aim toward more complete remissions and improved long-term disease control.

Disclosure of Potential Conflicts of Interest

No potential conflicts of interest were disclosed.

Authors' Contributions

Conception and design: A. Duensing
Development of methodology: D.J. Lee, K.R. Mehalek, K.R. Makielski, D.S. Seneviratne, M. Debiec-Rychter, A. Duensing
Acquisition of data (provided animals, acquired and managed patients, provided facilities, etc.): S. Boichuk, D.J. Lee, K.R. Mehalek, K.R. Makielski, A. Wozniak, D.S. Seneviratne, N. Korzeniewski, R. Cuevas, J.A. Parry, M.F. Brown, S.-F. Kuan, P. Schöffski, M. Debiec-Rychter, A. Duensing
Analysis and interpretation of data (e.g., statistical analysis, biostatistics, computational analysis): S. Boichuk, D.J. Lee, K.R. Mehalek, K.R. Makielski, A. Wozniak, D.S. Seneviratne, R. Cuevas, M.F. Brown, J.P. Zewe, P. Schöffski, A. Duensing
Writing, review and/or revision of the manuscript: S. Boichuk, D.J. Lee, A. Wozniak, J.P. Zewe, P. Schöffski, M. Debiec-Rychter, A. Duensing
Administrative, technical, or material support (i.e., reporting or organizing data, constructing databases): J.P. Zewe, T. Taguchi, P. Schöffski, M. Debiec-Rychter
Study supervision: M. Debiec-Rychter, A. Duensing

Acknowledgments

The authors thank J.A. Fletcher for sharing important reagents, C. Bakkenist and R. Sobol for help with the Comet assay, and S. Duensing for critically reading the manuscript and valuable discussions.

Grant Support

This work was supported by a Research Scholar Grant from the American Cancer Society (RSG-08-092-01-CCG; A. Duensing), The Life Raft Group (A. Duensing and M. Debiec-Rychter), the GIST Cancer Research Fund (A. Duensing), and an Undergraduate Research Grant of the Howard Hughes Medical Institute (D.J. Lee). A. Duensing is supported by the University of Pittsburgh Cancer Institute and in part by a grant from the Pennsylvania Department of Health. The Department specifically disclaims responsibility for any analyses, interpretations, or conclusions.

The costs of publication of this article were defrayed in part by the payment of page charges. This article must therefore be hereby marked *advertisement* in accordance with 18 U.S.C. Section 1734 solely to indicate this fact.

Received July 12, 2013; revised November 19, 2013; accepted November 21, 2013; published OnlineFirst January 2, 2014.

References

1. Hirota S, Isozaki K, Moriyama Y, Hashimoto K, Nishida T, Ishiguro S, et al. Gain-of-function mutations of c-kit in human gastrointestinal stromal tumors. Science 1998;279:577–80.
2. Demetri GD, Mehren von M, Blanke CD, Van den Abbeele AD, Eisenberg B, Roberts PJ, et al. Efficacy and safety of imatinib mesylate in advanced gastrointestinal stromal tumors. N Engl J Med 2002;347:472–80.
3. Rubin BP, Singer S, Tsao C, Duensing A, Lux ML, Ruiz R, et al. KIT activation is a ubiquitous feature of gastrointestinal stromal tumors. Cancer Res 2001;61:8118–21.

Published OnlineFirst January 2, 2014; DOI: 10.1158/0008-5472.CAN-13-1955

4. Heinrich MC, Corless CL, Duensing A, McGreevey L, Chen C-J, Joseph N, et al. PDGFRA activating mutations in gastrointestinal stromal tumors. Science 2003;299:708–10.
5. Verweij J, Casali PG, Zalcberg J, LeCesne A, Reichardt P, Blay JY, et al. Progression-free survival in gastrointestinal stromal tumours with high-dose imatinib: randomised trial. Lancet 2004;364: 1127–34.
6. Rock EP, Goodman V, Jiang JX, Mahjoob K, Verbois SL, Morse D, et al. Food and Drug Administration drug approval summary: sunitinib malate for the treatment of gastrointestinal stromal tumor and advanced renal cell carcinoma. Oncologist 2007;12:107–13.
7. Demetri GD, Reichardt P, Kang Y-K, Blay J-Y, Rutkowski P, Gelderblom H, et al. Efficacy and safety of regorafenib for advanced gastrointestinal stromal tumours after failure of imatinib and sunitinib (GRID): an international, multicentre, randomised, placebo-controlled, phase 3 trial. Lancet 2013;381:295–302.
8. Gramza AW, Corless CL, Heinrich MC. Resistance to tyrosine kinase inhibitors in gastrointestinal stromal tumors. Clin Cancer Res 2009;15:7510–8.
9. Wardelmann E, Thomas N, Merkelbach-Bruse S, Pauls K, Speidel N, Buttner R, et al. Acquired resistance to imatinib in gastrointestinal stromal tumours caused by multiple KIT mutations. Lancet Oncol 2005;6:249–51.
10. Antonescu CR, Besmer P, Guo T, Arkun K, Hom G, Koryotowski B, et al. Acquired resistance to imatinib in gastrointestinal stromal tumor occurs through secondary gene mutation. Clin Cancer Res 2005;11: 4182–90.
11. Dematteo RP, Heinrich MC, El-Rifai WM, Demetri G. Clinical management of gastrointestinal stromal tumors: before and after STI-571. Hum Pathol 2002;33:466–77.
12. Liu Y, Tseng M, Perdreau SA, Rossi F, Antonescu C, Besmer P, et al. Histone H2AX is a mediator of gastrointestinal stromal tumor cell apoptosis following treatment with imatinib mesylate. Cancer Res 2007;67:2685–92.
13. Bauer S, Parry JA, Mühlenberg T, Brown MF, Seneviratne D, Chatterjee P, et al. Proapoptotic activity of bortezomib in gastrointestinal stromal tumor cells. Cancer Res 2010;70:150–9.
14. dtp.nci.nih.gov [Internet]. Available from: http://dtp.nci.nih.gov
15. Edris B, Fletcher JA, West RB, van de Rijn M, Beck AH. Comparative gene expression profiling of benign and malignant lesions reveals candidate therapeutic compounds for leiomyosarcoma. Sarcoma 2012;2012:805614.
16. Taguchi T, Sonobe H, Toyonaga S-I, Yamasaki I, Shuin T, Takano A, et al. Conventional and molecular cytogenetic characterization of a new human cell line, GIST-T1, established from gastrointestinal stromal tumor. Lab Invest 2002;82:663–5.
17. Reynoso D, Nolden LK, Yang D, Dumont SN, Conley AP, Dumont AGP, et al. Synergistic induction of apoptosis by the Bcl-2 inhibitor ABT-737 and imatinib mesylate in gastrointestinal stromal tumor cells. Mol Oncol 2011;5:93–104.
18. Tuveson DA, Willis NA, Jacks T, Griffin JD, Singer S, Fletcher CD, et al. STI571 inactivation of the gastrointestinal stromal tumor c-KIT oncoprotein: biological and clinical implications. Oncogene 2001; 20:5054–8.
19. Bauer S, Duensing A, Demetri GD, Fletcher JA. KIT oncogenic signaling mechanisms in imatinib-resistant gastrointestinal stromal tumor: PI3-kinase/AKT is a crucial survival pathway. Oncogene 2007;26: 7560–8.
20. Duensing A, Medeiros F, McConarty B, Joseph NE, Panigrahy D, Singer S, et al. Mechanisms of oncogenic KIT signal transduction in primary gastrointestinal stromal tumors (GISTs). Oncogene 2004;23: 3999–4006.
21. Floris G, Debiec-Rychter M, Sciot R, Stefan C, Fieuws S, Machiels K, et al. High efficacy of panobinostat towards human gastrointestinal stromal tumors in a xenograft mouse model. Clin Cancer Res 2009; 15:4066–76.
22. Boichuk S, Parry JA, Makielski KR, Litovchick L, Baron JL, Zewe J, et al. The DREAM complex mediates GIST cell quiescence and is a novel therapeutic target to enhance imatinib-induced apoptosis. Cancer Res 2013;73:5120–9.
23. Boichuk S, Hu L, Hein J, Gjoerup OV. Multiple DNA damage signaling and repair pathways deregulated by simian virus 40 large T antigen. J Virol 2010;84:8007–20.
24. Gupta A, Roy S, Lazar AJF, Wang W-L, McAuliffe JC, Reynoso D, et al. Autophagy inhibition and antimalarials promote cell death in gastrointestinal stromal tumor (GIST). Proc Natl Acad Sci USA 2010; 107:14333–8.
25. Grohar PJ, Woldemichael GM, Griffin LB, Mendoza A, Chen QR, Yeung C, et al. Identification of an inhibitor of the EWS-FLI1 oncogenic transcription factor by high-throughput screening. JNCI 2011;103: 962–78.
26. Fujimoto S, Ogawa M. Antitumor activity of mitoxantrone against murine experimental tumors: comparative analysis against various antitumor antibiotics. Cancer Chemother Pharmacol 1982;8: 157–62.
27. Agaram NP, Besmer P, Wong GC, Guo T, Socci ND, Maki RG, et al. Pathologic and molecular heterogeneity in imatinib-stable or imatinib-responsive gastrointestinal stromal tumors. Clin Cancer Res 2007; 13:170–81.
28. de Hoon MJL, Imoto S, Nolan J, Miyano S. Open source clustering software. Bioinformatics 2004;20:1453–4.
29. Koller CA, Miller DM. Preliminary observations on the therapy of the myeloid blast phase of chronic granulocytic leukemia with plicamycin and hydroxyurea. N Engl J Med 1986;315:1433–8.
30. Alberts DS, Peng YM, Leigh S, Davis TP, Woodward DL. Disposition of mitoxantrone in cancer patients. Cancer Res 1985;45:1879–84.
31. Ehninger G, Proksch B, Heinzel G, Woodward DL. Clinical pharmacology of mitoxantrone. Cancer Treat Rep 1986;70:1373–8.
32. Bhalla K, Ibrado AM, Tourkina E, Tang C, Grant S, Bullock G, et al. High-dose mitoxantrone induces programmed cell death or apoptosis in human myeloid leukemia cells. Blood 1993;82: 3133–40.
33. Feldman EJ, Alberts DS, Arlin Z, Ahmed T, Mittelman A, Baskind P, et al. Phase I clinical and pharmacokinetic evaluation of high-dose mitoxantrone in combination with cytarabine in patients with acute leukemia. J Clin Oncol 1993;11:2002–9.
34. Zhang M, Mathur A, Zhang Y, Xi S, Atay S, Hong JA, et al. Mithramycin represses basal and cigarette smoke-induced expression of ABCG2 and inhibits stem cell signaling in lung and esophageal cancer cells. Cancer Res 2012;72:4178–92.
35. Van Dyke MW, Dervan PB. Chromomycin, mithramycin, and olivomycin binding sites on heterogeneous deoxyribonucleic acid. Footprinting with (methidiumpropyl-EDTA)iron(II). Biochemistry 1983;22: 2373–7.
36. Blume SW, Snyder RC, Ray R, Thomas S, Koller CA, Miller DM. Mithramycin inhibits SP1 binding and selectively inhibits transcriptional activity of the dihydrofolate reductase gene *in vitro* and *in vivo*. J Clin Invest 1991;88:1613.
37. Liu S, Wu L-C, Pang J, Santhanam R, Schwind S, Wu Y-Z, et al. Sp1/NF$_K$B/HDAC/miR-29b regulatory network in KIT-driven myeloid leukemia. Cancer Cell 2010;17:333–47.
38. Bauer S, Yu LK, Demetri GD, Fletcher JA. Heat shock protein 90 inhibition in imatinib-resistant gastrointestinal stromal tumor. Cancer Res 2006;66:9153–61.
39. Liu Y, Parry JA, Chin A, Duensing S, Duensing A. Soluble histone H2AX is induced by DNA replication stress and sensitizes cells to undergo apoptosis. Mol Cancer 2008;7:61.
40. Mitsui A, Sharp PA. Ubiquitination of RNA polymerase II large subunit signaled by phosphorylation of carboxyl-terminal domain. Proc Natl Acad Sci USA 1999;96:6054–9.
41. Stoimenov I, Schultz N, Gottipati P, Helleday T. Transcription inhibition by DRB potentiates recombinational repair of UV lesions in mammalian cells. PLoS ONE 2011;6:e19492.
42. Li TK, Liu LF. Tumor cell death induced by topoisomerase-targeting drugs. Annu Rev Pharmacol Toxicol 2001;41:53–77.
43. Kellner U, Sehested M, Jensen PB, Gieseler F, Rudolph P. Culprit and victim—DNA topoisomerase II. Lancet Oncol 2002;3:235–43.
44. Burgess DJ, Doles J, Zender L, Xue W, Ma B, McCombie WR, et al. Topoisomerase levels determine chemotherapy response *in vitro* and *in vivo*. Proc Natl Acad Sci USA 2008;105:9053–8.

Published OnlineFirst January 2, 2014; DOI: 10.1158/0008-5472.CAN-13-1955

45. Castedo M, Perfettini J-L, Roumier T, Andreau K, Medema R, Kroemer G. Cell death by mitotic catastrophe: a molecular definition. Oncogene 2004;23:2825–37.
46. Eilber FC, Rosen G, Forscher C, Nelson SD, Dorey FJ, Eilber FR. Surgical resection and intraperitoneal chemotherapy for recurrent abdominal sarcomas. Ann Surg Oncol 1999;6:645–50.
47. Maurel J, Martins AS, Poveda A, López-Guerrero JA, Cubedo R, Casado A, et al. Imatinib plus low-dose doxorubicin in patients with advanced gastrointestinal stromal tumors refractory to high-dose imatinib. Cancer 2010;116:3692–701.
48. Trent JC, Beach J, Burgess MA, Papadopolous N, Chen LL, Benjamin RS, et al. A two-arm phase II study of temozolomide in patients with advanced gastrointestinal stromal tumors and other soft tissue sarcomas. Cancer 2003;98:2693–9.
49. Pessetto ZY, Weir SJ, Sethi G, Broward MA, Godwin AK. Drug repurposing for gastrointestinal stromal tumor. Mol Cancer Ther 2013;12:1299–309.
50. clinicaltrials.gov [Internet]. [cited 2013 Sep 18]. Available from: http://clinicaltrials.gov.
51. Snyder RC, Ray R, Blume S, Miller DM. Mithramycin blocks transcriptional initiation of the c-myc P1 and P2 promoters. Biochemistry 1991;30:4290–7.
52. Remsing LL, Bahadori HR, Carbone GM, McGuffie EM, Catapano CV, Rohr J. Inhibition of c-src transcription by ithramycin: structure–activity relationships of biosynthetically produced mithramycin analogues using the c-src promoter as target. Biochemistry 2003;42:8313–24.
53. Rossi F, Yozgat Y, de Stanchina E, Veach D, Clarkson B, Manova K, et al. Imatinib upregulates compensatory integrin signaling in a mouse model of gastrointestinal stromal tumor and is more effective when combined with dasatinib. Mol Cancer Res 2010;8:1271–83.
54. Ho AD, Seither E, Ma DD, Prentice HG. Mitozantrone-induced toxicity and DNA strand breaks in leukaemic cells. Br J Haematol 1987;65:51–5.
55. Lee MJ, Ye AS, Gardino AK, Heijink AM, Sorger PK, MacBeath G, et al. Sequential application of anticancer drugs enhances cell death by rewiring apoptotic signaling networks. Cell 2012;149:780–94.